Effect of aqueous corrosion on the high cycle fatigue strength of a martensitic stainless steel

M. El May [1,a] , T. Palin-Luc [1,b] , N. Saintier [1,c] , O. Devos [2,d]

[1] Arts et Métiers ParisTech, I2M, CNRS, Esplanade des Arts et Métiers, 33405 Talence, France

[2] Université de Bordeaux, I2M, CNRS, 351 Cours de la libération, 33405 Talence, France

[a] mohamed.elmay@ensam.eu, [b] thierry.palin-luc@ensam.eu, [c] nicolas.saintier@ensam.eu,
[d] o.devos@lmp.u-bordeaux1.fr

Abstract

This study is devoted to the investigation of the aqueous corrosion effect on the high cycle fatigue (HCF) strength of a martensitic stainless steel used in aeronautic applications. HCF tests (between 10^5 and 10^7 cycles) were carried out in two environments: (i) in air and (ii) in a 0.1 M NaCl aqueous solution (pH = 6) with two load ratios (R=-1 and 0.1). The corrosion fatigue strength at 10^7 cycles was found to be 50% the fatigue strength in air. Surface crack initiation was observed in air, while in solution crack initiated at corrosion pits. Electrochemical behaviour of passive film was investigated during in situ fatigue tests in NaCl solution by monitoring the free potential and galvanostatic impedance EIS tests. Based on fractography analysis and electrochemical test results, fatigue crack initiation mechanisms in air and in NaCl solution were investigated. A scenario of fatigue crack initiation is proposed based on physical evidences. Local passive film ruptures are the principal cause of the corrosion fatigue crack initiation. This scenario implies combined processes of local passive film rupture (induced by the cyclic loading) stress assisted corrosion and enhanced pitting development. This aspects will be discussed by comparing the characteristic time of repassivation of the steel to the mechanical characteristic times (loading frequency, plasticity development). No loading frequency effect was observed between 10 and 120 Hz because the characteristic time of repassivation of the steel is very low compared to the period of the cyclic loading. But the existence of threshold stress amplitude has been shown, below which there is no passive film failure under cyclic loading, and, consequently no corrosion fatigue crack initiation after 10^7 cycles.

Introduction

Designing structures against corrosion fatigue is a key problem for many engineering structures in particular in transportation and civil engineering where structures evolve in complex environmental conditions of temperature and humidity. For aeronautic structures, corrosion fatigue processes can particularly develop in confined areas were, in addition, non-destructive damage detection techniques can hardly be applied. For these reasons, aeronautic materials with high specific strength are being developed to fulfil ever increasing requirements in terms of corrosion fatigue resistance.

The combined influence of corrosion and cyclic loading is known to affect the mechanical properties of metallic alloys and have been shown to initiate cracks from corrosion induced surface defects. Corrosion fatigue in NaCl aqueous solutions have been studied by numerous researchers [1-6]. A number of crack mechanisms have been suggested: these include the competition between pit growth and short crack growth [1], preferential dissolution of plastically deformed material [2], local rupture of passive film by persistent slip bands (PSB) [3], hydrogen embrittlement in the cathodic domain and deformation / corrosion synergy effects [4]. However, all these mechanisms depend on the experimental conditions (loading frequency, stress strain level, environment, electrochemical potential value...), and on material properties (cleanness, segregation …). Some works noted that corrosion produces greater damage at low frequency than under a high frequency [1, 5], because the time exposure in corrosive environment at high stress level (respectively

low) is longer at low frequency than at high frequency. However, this is not always true. For instance, Palin-luc et al. [6] have shown on a hot rolled low-alloy steel grade R5, a very important effect of corrosive environment (in 3 % NaCl aqueous solution named A3 sea water) on the fatigue strength in the gigacycle regime during tests at very high frequency (20 KHz). This shows that the frequency effect in corrosion fatigue is not very well understood.

The purpose of this paper is to understand the initiation mechanism of corrosion fatigue crack on a martensitic stainless steel loaded in the HCF domain (10^5 to 10^7 cycles). The corrosive environment is NaCl aqueous solution. To investigate the corrosion fatigue phenomenon, in-situ electrochemical impedance spectroscopy (EIS) tests were carried out during corrosion fatigue tests under potentiostatic measurement. These experiments and SEM observations of the fracture surface of the specimens allow us to understand the corrosion fatigue damage phenomena and to propose a fatigue crack initiation scenario based on physical evidences. Furthermore, the effect of the loading frequency was investigated with two loading frequencies (10 Hz and 120 Hz) leading to realistic fatigue test duration for 10^7 cycles.

Material and experimental conditions

Material

The investigated material is a rolled martensitic stainless steel (X12CrNiMoV12-3) with a high specific strength developed for aeronautic applications. Its chemical composition and mechanical properties under quasi-static monotonic tension are shown in Tables 1 and 2.

Table 1. Chemical composition of the X12CrNiMoV 12-3 steel (wt %, Fe balance)

C	Cr	Ni	Mo	V
0.12	12	3	1.6	0.3

Table 2: Mechanical properties of the X12CrNiMoV 12-3 steel under monotonic quasi-static tension

E (GPa)	Rm (MPa)	$Rp_{0.2}$ (MPa)	A (%)
211	1430	1040	15

The microstructure of this steel is completely martensitic as shown in Fig. 1 (residual austenite content is less than 1 %). Austenitic grains have equiaxed structure and the grain size is about 100µm. The microstructure is free of visible inclusion in the 10 µm shown range.
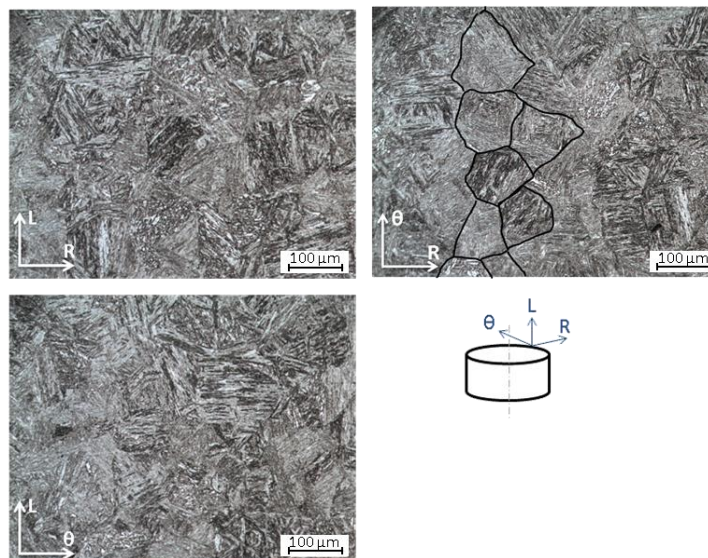

Fig.1. X12CrNiMoV 12-3 microstructure after heat treatment

Fatigue tests conditions and electrochemical measurement technique

Fatigue tests were carried out in air and in corrosive 0.1 M NaCl + 0.044 M Na$_2$SO$_4$ aqueous solution. Fatigue tests in air were performed on 8 mm diameter specimens with a theoretical stress concentration factor in tension Kt = 1.04. Corrosion fatigue tests in aqueous solution were carried out on 8 mm diameter cylindrical specimens (Kt =1.04). The roughness of the area of interest was less or equal to Ra = 0.1 μm for all the specimens. All the fatigue tests were carried out under axial loading and load controlled under free electric potential. Except for investigating the frequency effect, all the fatigue tests were performed at 120 Hz with a resonant electromagnetic fatigue testing machine (Vibrophore type). The stop criterion was a loading frequency drop of 0.7 Hz that corresponds to a technical fatigue crack with typical surface length of 5 mm and depth of 2 mm. For testing at 10 Hz and investing the effect of the loading frequency a servo-hydraulic fatigue testing machine was used.

An electrochemical corrosion cell was developed and made at the laboratory (compatible with both the vibrophore and the servo-hydraulic testing machine). That allows in-situ fatigue testing in aqueous corrosive environment. The specimens were electrically isolated from the frame of the fatigue testing machine. The whole gauge section (area of interest) of the specimen was electrochemically monitored using a potentiostatic/galvanostatic device. A three electrodes cell was used for the electrochemical investigation with a saturated calomel electrode (SCE) as reference maintained at a constant distance of 3 mm from the specimen surface, a platinum counter electrode (CE) and the specimen as working electrode (WE) (Fig. 2).

The electrochemical investigation was carried out in steady state and in transient regimes. Two electrochemical techniques were used in this study: the voltammetry and the electrochemical impedance spectroscopy (EIS). This latter, which is a dynamic technique, is well known to analyse the electrochemical mechanism occurring at the interface between electrode and solution [7]. A galvanostat leads a stationary zero current to be applied at the working electrode (the specimen) corresponding to open circuit potential (OCP). Then, a frequency response analyser (FRA) imposes a small amplitude of sine wave current modulation (6 μA) scanning the frequencies from the high values (100 Hz) up to smaller one (0.1 Hz). The high frequency range provides information concerning the passive film and/or the kinetic of the corrosion process whereas the low frequency domain characterises the slow processes such as the diffusion of ionic species in the solution from or toward the electrode surface. During the corrosion fatigue tests, the impedance measurements were performed at the open circuit potential (OCP) every 30 minutes in order to investigate the electrochemical behaviour versus time.
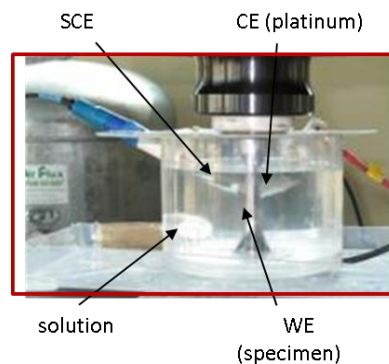

Fig. 2. In-situ corrosion fatigue cell with potentiostatic measurements.

Results and discussion

S-N curves in air and in NaCl aqueous solution

The S-N curves of the X12CrNiMoV12-3 under fully reversed tension in air and in aqueous solution are shown in figure 3, for two loading ratio R=-1 and R=0.1. These curves are normalized by the median fully reserved fatigue strength at 10^7 cycles ($\sigma^D_{R=-1}$). The results show a significant decrease of the fatigue

strength in corrosive aqueous NaCl solution 0.1 M compared to the fatigue in air. The median fatigue strength at 10^7 cycles in aqueous solution decreases of 33 % compared to the fatigue strength in air. Some corrosion fatigue tests in aqueous solution without NaCl were carried out, to understand the role of chloride. Similar to corrosion fatigue test in (0.1 M NaCl + 0.044 M Na_2SO_4) aqueous solution, the results show a significant decreasing of the corrosion fatigue strength in 0.1 M Na_2SO_4 aqueous solution and in distilled water compared to the fatigue in air (figure 3-b). SEM observations show that fatigue cracks initiated at surface corrosion defects in all aqueous testing solutions (0.1 M NaCl + 0.044 M Na_2SO_4, 0.1 M Na_2SO_4 and distilled water). For the fatigue test in air, fatigue crack initiation areas are located at the specimen surface.

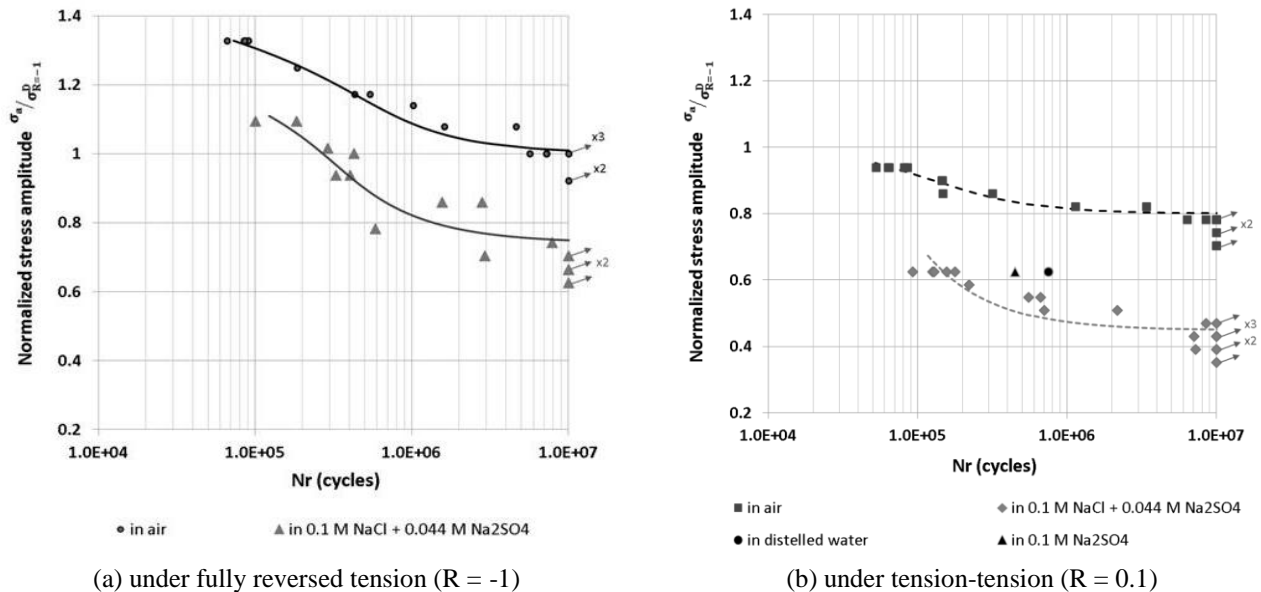(a) under fully reversed tension (R = -1) (b) under tension-tension (R = 0.1)

Fig. 3: Median S-N curves (survival probability Ps = 0.5) in air and in aqueous solutions at 120 Hz

We conclude that the corrosive effect (depassivation of the material) is not dependent on the chloride environment content only. Because in 0.1 M Na_2SO_4 solution and in distilled water the decreasing of the fatigue strength is important too.

Effect of cyclic loading on the free potential of the metal

Electrochemical tests without any mechanical loading allowed us to identify the passive region and free corrosion potential of X12CrMoV 12-3 steel. Passive region extends from -250 mV/SCE to 300 mV/SCE. Fig. 4 shows a linear scan voltammetry test with a scan rate 10 mV/s (from -1 V/SCE to 0.6 V/SCE).
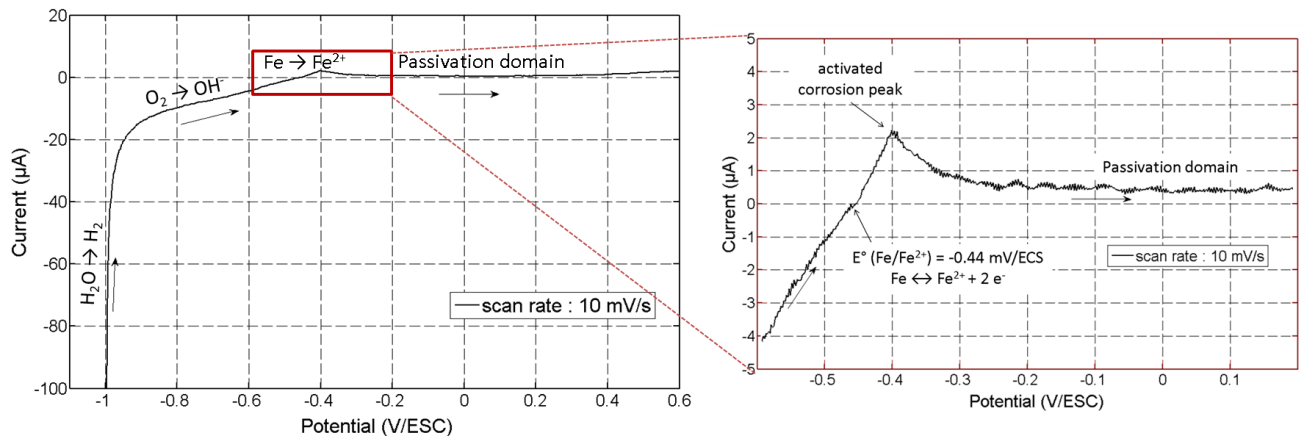

Fig. 4. Linear scan voltammetry test on a specimen without cyclic stress in 0.1 M NaCl + 0.044 M Na_2SO_4

An activated corrosion peak of ferrous around -400 mV/SCE can be noted. Free corrosion potential was recorded during cyclic loading (corrosion fatigue tests) in the same environment (0.1 M NaCl + 0.044 M Na2SO4 aqueous solution). Under cyclic loading, free potential decreased around "-400 mV/SCE" (Fig. 5). This value corresponds to the activated corrosion peak observed in linear scan voltammetry. For the corrosion fatigue test in 0.1 M Na2SO4 aqueous solution without chlorides free potential decreased also around "-400 mV/SCE" under cyclic loading. The concentration of Na_2SO_4 (0.1 M) was chosen to have the same number of ions as in the (0.1 M NaCl + 0.044 M Na_2SO_4) aqueous solution. Free potential decrease around "-400 mV/SCE" was observed for all the corrosion fatigue tests excepted for specimens which did not fail in (0.1 M NaCl + 0.044 M Na_2SO_4) aqueous solution after 10^7 cycles under the median fatigue strength in aqueous solution (Fig. 3).
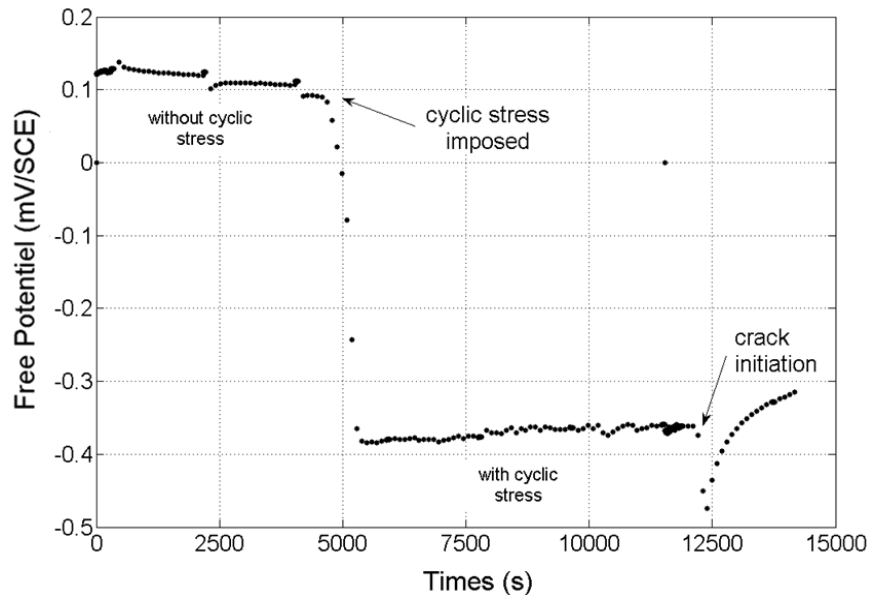
$$R = 0.1 \; ; \; \text{in } 0.1 \text{ M NaCl} + 0.044 \text{ M Na}_2\text{SO}_4 \; ; \; \frac{\sigma_a}{\sigma_{R=-1}^D} = 0.55 \; ; \; f = 120 \text{ Hz} \; ; \; N = 9.2 \; 10^5 \text{ cycles}$$

Fig. 5. Free corrosion potential evolution during corrosion fatigue test of specimen

Electrochemical impedance spectroscopy (EIS) measurement during fatigue tests

Usually equivalent circuit modelling of EIS data is used to extract physically based properties of the electrochemical system by modelling the impedance data in terms of an equivalent electrical circuit. A resistance in parallel with capacitance was classically considered in particular to investigate the high frequency domain of electrochemical impedance measurement. The low frequencies of EIS were investigated by low time constants such as adsorption mechanism or diffusion process. Because we are dealing with a real system that does not necessarily behave ideally (processes that occur are distributed in time and space), specialized circuit elements are usually considered. These include a constant phase element (CPE) to take into account the special distribution of the capacitances on the electrode surface [7, 8]. The equivalent circuit chosen for modelling the corrosion fatigue process is shown in Fig. 6.
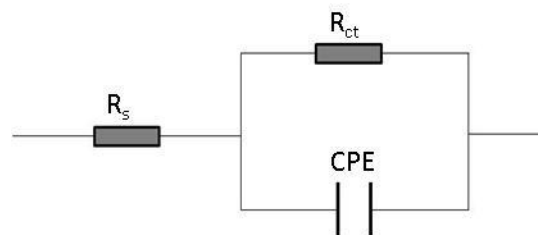

Fig. 6. Equivalent circuit of impedance diagram

This simple model represents the Faraday's reaction at high frequency (of the alternative current). The cell impedance analogue contents solution resistance "R_s" in series with capacitance "CPE" shunted by a charge-transfer resistance "R_{ct}". A fitting program (Zsimwin) was used to provide the coefficient values of the CPE, R_{ct} and R_s. To understand such behaviour, the fitted values of the resistance and the capacitances are plotted for an exposed surface of 5 cm^2 in Fig. 7.

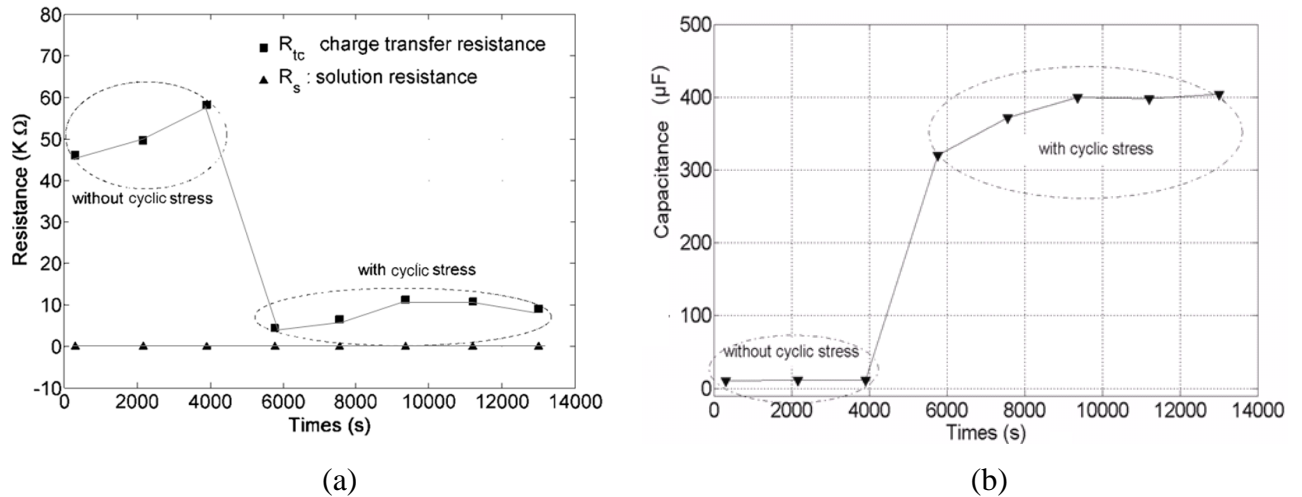(a)   (b)

Fig. 7. Evolution of (a) the charge-transfer resistance and (b) the capacitance (CPE) of the model in Fig. 6 before any cyclic loading and during cyclic loading

Two regimes were clearly observed: without cyclic stress and with cyclic stress. Without cyclic stress, a very high resistance and a weak capacitance were measured. This result denotes the presence of a resistance material due to the presence of its protective passive film. After the cyclic stress beginning, the resistance strongly decreases and the capacitance increases. This shows that the material is more conductive due to the local rupture of the passive film. In that case, the measured resistance corresponds to the electronic charge transfer process of the metal dissolution [9]. Additionally, it has to be noticed that the corrosive attack on the surface of all the specimens tested in corrosion fatigue conditions was produced in small areas scattered all over the specimen surface. There was no generalized corrosion.

Corrosion fatigue crack initiation mechanism

The previous analysis and observations are physical evidences that corrosion fatigue crack initiation for the tested stainless steel X12CrNiMoV12-3 is related to the local fracture of the passive film due to cyclic stress strain. These local ruptures of the passive film and the shift of the free potential in 0.1 M Na_2SO_4 and in (0.1 M NaCl + 0.044 M Na_2SO_4) aqueous solutions can be reported to (i) the appearance of slip bands on the surface in the early stage of deformation and/or (ii) the variation of passive film thickness. Furthermore, SEM observation of the surface of cracked specimen tested under corrosion fatigue revealed persistant slip bands which are responsible of the passive film local ruptures. Inded, Auger probe measurments of the passive film thickness where carried out on the X12CrNiMoV12-3 steel. The thickness is around 3nm in air and 7nm in (0.1 M NaCl + 0.044 M Na_2SO_4) aqueous solutions. The typical high of extrusion at the surface of steel with PSB is greater than the passive film thickness: between 10 and 200 nm in PH 13-8 Mo martensitic stainless steel tested at 0.6% strain amplitude and 10 nm at 0.4% strain amplitude and surface streaks are 4 nm deep under 0.4% strain amplitude [10]. Thus the passive film can not accommodate so strong local deformation. A schematic illustration, of this corrosion fatigue process is illustrated in Fig.8. In this process stress level (amplitude and mean value) and load frequency play an important role to maintain the depassivation of the material.
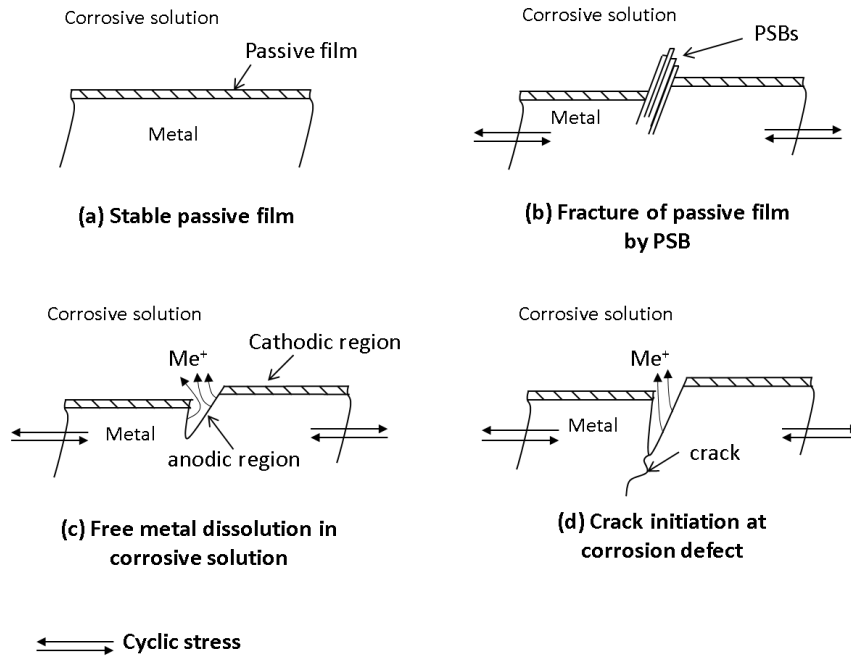
Fig. 8. Scenario of corrosion fatigue crack initiation at pits on martensitic stainless steel X12CrNiMoV 12-3 under loading frequency of 120 Hz in HCF regime (10^5-10^7 cycles)

About the loading frequency

The possible effect of the loading frequency in corrosion fatigue is related to the repassivation rate after local ruptures of the passive film. The repassivation rate of the X12CrNiMoV12-3 metal was determined studying the evolution of open circuit potential (OCP) after the depassivation under cyclic stress in a corrosive environment with 0.1 M NaCl and 0.044 M Na_2SO_4. The repassivation rate (OCP needs about 3 days to enjoy 100 mV) is significantly lower than the characteristic time of the cyclic stress strain at the loading frequency (1/120 = 8.3 ms). Furthermore, Table 3 shows in the same conditions that under a loading frequency of 10 Hz failure occurred after around 10^5 cycles. This fatigue life is similar to the number of cycles to crack initiation with a loading frequency of 120 Hz. As a matter of fact, the load frequency ranging from 10 Hz to 120 Hz has no significant effect on the lifetime in corrosion fatigue under a normalized stress amplitude $\sigma_a / \sigma^D_{R=-1} = 1.1$ (R=-1) in aqueous solution 0.1 M NaCl + 0.044 M Na_2SO_4 (Table3). For the steel studied in this paper, it is clear that in HCF regime there is no effect, on the corrosion fatigue life, of the loading frequency (between 10 and 120 Hz).

Table 3. Results of corrosion fatigue tests at 2 different loading frequencies (120 Hz and 10 Hz) at R= -1

specimen Number	Loading frequency (Hz)	Normalized stress amplitude	Corrosion solution	Cycles to failure
21	120	$\sigma_a / \sigma^D_{R=-1} = 1.1$	0.1 M NaCl + 0.044 Na_2SO_4	1.83×10^5
22				1.77×10^5
31	10			7.6×10^4
32				1.14×10^5

Conclusion and prospects

In this paper fatigue crack initiation process of X12CrNiMoV12-3 in air at 120 Hz was identified. It was also shown that there is a significant decrease of the fatigue strength (in HCF regime) under corrosion for all the aqueous environments investigated at 120Hz (0.1 M NaCl + 0.044 M Na_2SO_4, 0.1 M Na_2SO_4 and distilled water) compared to the fatigue in air. Electrochemical behaviour of X12CrNiMoV12-3 was studied to identify the effect of cyclic stress on the passive film. The potential decreased tremendously about –

400 mV/ES when cyclic stress strain is applied in all the aqueous environments investigated (0.1 M NaCl + 0.044 M Na_2SO_4 and 1 M Na_2SO_4). This phenomenon was related to the fracture of the surface passive film identified by galvanostatic impedance measurements (EIS). However, for R=0.1 at the relatively low normalized stress amplitude ($\sigma_a / \sigma^D_{R=-1} \cong 0.4$; R = 0.1) the potential decrease was not observed and there was no crack initiation after 10^7 cycles. It can be concluded that at very low stress amplitudes the passive film is stable and protects the material against corrosion (up to 10^7 cycles at least). Based on these physical evidences, a scenario of corrosion fatigue crack initiation mechanisms was proposed. In this process, stress level (amplitude and means value) and loading frequency have an important role to maintain the depassivation of the material. Futhermore, it has been shown that for R = -1 the load frequency ranging from 10 Hz to 120 Hz has no appreciable effect on the corrosion fatigue crack initiation life at a normalized stress amplitude of $\sigma_a / \sigma^D_{R=-1} = 1.1$ (R = -1) in (0.1 M NaCl + 0.044 M Na_2SO_4) aqueous solution.

Acknowledgments

References

[1]   Y. Kondo, ''Prediction of fatigue crack initiation life based on pit growth'', Corrosion Vol. 45, pp. 7-11, (1979)

[2]   S. Xu, X.Q. Wu, E.H. Han, W. Ke, Y. Katada ''Crack initiation mechanisms for low cycle fatigue of type 316Ti stainless steel in High temperature water'', Mat. Sci. and Eng. A, Vol. 490, pp. 16-25 (2008)

[3]   C. Laird, D. J. Duquette, ''Mechanisms of fatigue crack nucleation'', In Corrosion fatigue: chemistry, mechanics and microstructure, O. Devereux, A.J. McEvily and R.W. Stachle Editors, Nat. Ass. Corr. Engng (NACE) – 2, p. 88, (1973)

[4]   R. Pelloux and J.-M. Genkin ''Chapitre 10: Fatigue-corrosion'', in C. Bathias and A. Pineau, ''Fatigue des matériaux et des structures'', Vol. 2, Ed. Hermès, Paris, pp. 141-152 (2008)

[5]   T. Palin-Luc, Ruben Pérez-Mora, Claude Bathias, Gonzalo Domínguez, Paul C. Paris, Jose Luis Arana, ''Fatigue crack initiation and growth on a steel in the very high cycle regime with sea water corrosion.'', Engng. Fract. Mech., Vol. 77, pp. 1953-1962, (2010)

[6]   R. Ebara al. "Corrosion fatigue behaviour of 13Cr stainless steel and Ti-6Al-4V ultrasonic frequency", Fatigue ultrasonore, TMS (1980)

[7]   D. J. McAdam, "Corrosion Fatigue of Metals", Jr. Trans. Am. Soc. Steel Treat., 11, pp. 355-79 (1927)

[8]   O. Devos, G. Gabrielli, B. Tribollet, "Simultaneous EIS and in situ microscope observation on partially blocked electrode application to scale electrodeposition", Electrochimica Acta, Vol 51, pp. 1413-1422 (2006)

[9]   G.J. Brug, A.L.G. Van Den Eeden, M. Sluyters-Rehbach, J.H. Sluyters, "The analysis of electrode impedances complicated by the presence of a constant phase element" J. Electroanal. Chem., 176, p. 275 (1984)

[10]   O. Ferraz, E. Cavalcanti and A.R. Di Sarli, "The characterization of protective properties for some naval steel/polimeric coating/3% NaCl solution systems by EIS and visual assessment", Corrosion Science, Vol. 37, pp. 1267–1280 (1995)

[11]   C Liu, Q Bi and A Matthews, "EIS comparison on corrosion performance of PVD TiN and CrN coated mild steel in 0.5 N NaCl aqueous solution", Corrosion Science, Vol 43, pp. 1953–1961 (2001)

[12]   L. Cretegny and A. Saxena, "Evolution of surface deformation during fatigue of PH 13-8 Mo stainless steel using atomic force microscopy", Fatigue Fract. Engng. Mater. Struct. 25, pp. 305-314 (2002)